Journal of Hydrology 526 (2015) 136–150

Contents lists available at ScienceDirect

Journal of Hydrology

journal homepage: www.elsevier.com/locate/jhydrol

Probabilistic forecasting of drought class transitions in Sicily (Italy) using Standardized Precipitation Index and North Atlantic Oscillation Index

Brunella Bonaccorso [a,*], Antonino Cancelliere [b,1], Giuseppe Rossi [b,1]

[a] Department of Civil, Computer, Construction and Environmental Engineering and Applied Mathematics, University of Messina, C.da di Dio, 98166, S. Agata, Messina, Italy
[b] Department of Civil Engineering and Architecture, University of Catania, Via Santa Sofia, 64 – 95123 Catania, Italy

ARTICLE INFO

Article history:
Available online 7 February 2015

Keywords:
Drought
Probabilistic forecasting models
Transition probability
SPI
NAO
Sicily (Italy)

SUMMARY

Since the mid-90s the Standardized Precipitation Index (SPI) has found widespread use to monitor drought periods at different time scales. Recently, some efforts have been made to analyze the role of SPI for drought forecasting, as well as to estimate transition probabilities between SPI drought classes.

In the present paper probabilistic models for short and middle term forecasting of SPI drought class transition probabilities are presented and extended in order to include information provided by an exogenous variable, such as an index of large scale atmospheric circulation pattern like, for instance, the North Atlantic Oscillation index (NAO). In particular, the proposed models result from evaluating conditional probability of future SPI classes with respect to current SPI (and NAO) classes or current SPI (and NAO) values, under the hypothesis of multivariate normal distribution of the underlying joint variables.

SPI series are computed on average areal precipitation in Sicily region (Italy). As a significant negative correlation exists between NAO and SPI series in Sicily during recent decades, the proposed models are calibrated on the period from 1979 to 2008. Both SPI and NAO values are categorized in four classes. Transition probabilities to future SPI classes are evaluated based on SPI and NAO current classes or values and compared to the corresponding probabilities when NAO is neglected. Results indicate that drought transition probabilities in Sicily are generally affected by NAO index. In particular, transition probabilities related to persisting or worsening drought conditions significantly increase as NAO index tends toward extremely positive values. On the other hand transition probabilities to a less severe drought class decrease as NAO values increase.

Furthermore, application of a simple score approach to quantitatively assess the skill in forecasting of the proposed models shows that assessing transition probabilities to future SPI classes from current SPI and NAO values leads to better results than considering current classes.

1. Introduction

It is largely recognized that an effective mitigation of the most adverse drought impacts is possible by capitalizing on the usually significant delay between drought inception (i.e. meteorological drought) and the moment when its consequences are perceived by the water supply systems and the end-users (i.e. socio-economic impacts of drought). To this end, a drought monitoring and forecasting system, able to promptly warn against an incipient phenomenon and to follow its evolution in space and time, represents the prerequisite for a successful mitigation strategy (Rossi, 2003).

Many statistical and non statistical techniques have been proposed to forecast droughts (Bonaccorso et al., 2012 and references therein). Regardless of the specific methodology, a distinction can be made with reference to the objective of the forecast. On the one hand, the interest may lie in forecasting future values of the hydrometeorological variable or drought index under investigation. On the other hand, the objective may lie in determining transition probabilities from a given current drought class (expressed in terms of a drought severity variable or index) to another one in the future.

Several forecasting techniques have been proposed to assess the probable evolution of drought related hydrometeorological variables or drought indices, such as: time series modeling (Rao and Padmanabhan, 1984; Mishra and Desai, 2005; Cancelliere et al., 2007; Modarres, 2007; Fernandez et al., 2009; Durdu, 2010; Han et al., 2010), black-box models (Mishra and Desai,

* Corresponding author. Tel.: +39 090 3977561; fax: +39 090 3977480.
E-mail addresses: bbonaccorso@unime.it (B. Bonaccorso), acance@dica.unict.it (A. Cancelliere), grossi@dica.unict.it (G. Rossi).
[1] Tel.: +39 095 7382718; fax: +39 095 7382748.

http://dx.doi.org/10.1016/j.jhydrol.2015.01.070
0022-1694/

2006; Morid et al., 2007; Bacanli et al., 2009; Barua et al., 2012; Belayneh et al., 2014) and hybrid models (Kim and Valdes, 2003; Mishra et al., 2007; Farokhnia et al., 2011; Ozger et al., 2012).

With reference to the forecasting of drought class transition probabilities, most of the literature focuses on some drought indices, such as the Palmer index (Palmer, 1965) or the Standardized Precipitation Index (SPI) (McKee et al., 1993). In particular, since the early paper by Gabriel and Neumann (1962), Markov models have been largely applied to evaluate drought class transition probabilities. For instance, a non homogeneous Markov chain model has been applied by Lohani and Loganathan (1997) and Lohani et al. (1998) to drought classes identified by means of the Palmer index. Paulo and Pereira (2007) used homogeneous Markov models to predict drought class transitions probabilities of SPI at 12-month time scale. The lag-1 Markov hypothesis for SPI series has been questioned by Cancelliere et al. (2007), who derived approximate analytical expressions for SPI drought class transition probabilities by assuming a multivariate normal distribution for SPI time series. More specifically, in their study the auto-covariance matrix of SPI values is expressed as a function of the statistics of the underlying monthly precipitation process, assumed serially independent and normally distributed.

Besides Markov chains, other models have been employed to estimate drought class transition probabilities. Paulo et al. (2005) used 2-D loglinear models to fit drought class transitions matrices constructed for several sites in southern Portugal. Moreira et al. (2006) applied a loglinear modeling approach to investigate differences in SPI drought class transitions with reference to three different periods between 1932 and 1999, in order to detect possible trends in time evolution of droughts which could be related to climate change. Moreira et al. (2008) extended the work of Paulo et al. (2005) using the same drought classification and 3-D loglinear models to predict drought class transitions one month ahead, given the drought class for the last two months, which also allows for extending the prediction to two months ahead. Kavalieratou et al. (2012) used a 3-D loglinear models approach for short-term forecast

Table 1
Main studies investigating the link between winter NAO and drought conditions in Europe and the Mediterranean region.

Authors	Study area	Investigated variables	Methodology	Main findings
Cullen and deMenocal (2000)	Eastern Mediterranean	Winter station averaged normalized temperature and precipitation series and DJFMA average streamflow of the Euphrates and Tigris rivers	Pearson's correlation analysis	Significant correlation with NAO is detected, with temperature and precipitation series showing decreasing trends during the 1980s, when NAO was persistently positive
Wedgbrow et al. (2002)	England and Wales	Summer Palmer Drought Severity Index (PDSI) and monthly reconstructed river flows	Spearman Rank correlation analysis; Split sample (composite) analysis for monthly river flows; Coherence testing/ index of forecast potential (IFP)	Positive winter NAO phases are associated with negative PDSI in summer across the eastern parts of the British Isles. Winter NAO phases may also precede below-average autumn river flows in Southeastern England
Türkes and Erlat (2003)	Turkey	Annual and seasonal normalized precipitation anomaly series	Pearson's correlation coefficient *r*; Composite analysis	Annual and seasonal precipitation are mostly characterized by wetter than the long-term average conditions during negative NAO phase, whereas positive NAO responses mostly exhibit drier than the long-term average conditions, except in summer
Muñoz-Diaz and Rodrigo (2004)	Spain	Regionalized precipitation classified into three categories: drought, normal or abundant	Analysis of changes of the empirical distribution of precipitation anomalies corresponding to positive, neutral and negative NAO phases	Positive NAO has an influence on the probability of drought all over Spain, while negative NAO affects the probability of abundant rainfall over the western area
Van der Schrier et al. (2006)	Europe	Summer self calibrated PDSI (Sc-PDSI)	Spatial correlation analysis	The most positive correlations are found in Western Scotland and Southern Norway. The most negative correlations are found in large areas over Spain
Lopez-Moreno et al. (2007)	Tagus river basin (Central Iberia)	Regional monthly precipitation, river discharge, reservoir storage and reservoir release	Comparison between normalized monthly values of the hydrological variables during positive and negative NAO years with the monthly values during normal NAO years and years of opposite NAO sign	Positive NAO years result in reduced water availability, whereas negative NAO years result in increased water availability
Lopez-Moreno and Vicente-Serrano (2008)	Europe	Gridded Standardized Precipitation Index (SPI) at different time scales	Spatial and temporal analysis of regionalized SPI response to positive and negative NAO phases	SPI dry/wet conditions occur during the positive/negative NAO phases over Southern Europe, whereas the opposite pattern occurs in Northern Europe
Brandimarte et al. (2011)	Southern Italy and Nile Delta (Egypt)	Winter precipitation, river flow and temperature	Pearson's correlation analysis	Negative correlation is found in most of the southern Italy, while low positive correlation is found in Eastern Sicilia and Nile Delta
Vicente-Serrano et al. (2011)	Mediterranean Region	Standardized Precipitation Evapotranspiration Index (SPEI)	Composite analysis	Outstanding influence of positive and negative phases of winter NAO is ascertained on drought conditions during the succeeding months
Wang et al. (2011)	Europe	Sc-PDSI	Coupled Manifold Technique	NAO regime over the Mediterranean modulates summer climate over Europe through controlling winter precipitation. A positive phase of NAO tends to generate the possibility of a hot and dry summer or vice versa

of drought class transitions in the Aison River Basin (Greece), based on the SPI values computed on a 12-month time scale.

Despite such efforts, forecasting when a drought is likely to begin or to come to an end is still a difficult task. Namias (1985) argues that drought is associated with persistent or persistently recurring atmospheric circulation patterns. Indeed, the link between changes in a number of large scale atmospheric circulation patterns and surface climate variability in many regions of the world has been largely documented by many studies during the last decades. Changes in climate variables, in turn, may reflect on the spatio-temporal variability of droughts.

Recently, important progress is being made in relation to the possibility of using information provided by some atmospheric circulation patterns, such as El Nino Southern Oscillation (ENSO) (Ropelewski and Halpert, 1987) and the North Atlantic Oscillation (NAO) (Hurrell, 1995), as a support to drought forecasting. Several studies have established links between NAO and climate in Europe and the Mediterranean basin. A summary of some recent studies which confirm the influence of positive winter NAO on drought conditions in Europe is tabulated in Table 1.

In spite of such promising results, only a few studies have investigated whether encompassing the influence of NAO, or of any other large scale climatic patterns data, into the models structure improves drought forecasting.

Cutore et al. (2009) have developed a forecasting model of Palmer Hydrological Drought Index (PHDI) series in Sicily (Italy) based on artificial neural networks by including information from NAO and the European Blocking (EB). Results indicate a better performance of the forecasting model in predicting winter and autumn PHDI values when NAO and, mainly, EB are taken into account.

Jamshidi et al. (2011) apply a Multi Layer Perceptron networks (MLPs) to forecast quantitative SPI values at five synoptic stations in Iran. The proposed models were built by using antecedent SPI and precipitation, as well as antecedent NAO and Southern Oscillation Index (SOI) as input values. The authors have found that the addition of NAO and SOI values as input variables to the MLPs improves the prediction efficiency of their models. Chen et al. (2013) have proposed a probabilistic drought forecasting model to forecast SPI at 3-month time scale in Southern Taiwan one-month ahead, by making use of ENSO index, based on sea surface temperature (SST) in the Eastern Pacific. The model is built upon empirical transition probability matrices of SPI state and SST state at different time horizons. Results reveal that the model using the transition probability matrix of SPI and ENSO-SST at the same month perform better than the one which considers SST at previous month with respect to SPI.

Santos et al. (2014) have developed a model to forecast spring SPI at 6-month time scale in mainland Portugal, based on artificial neural networks incorporating information on NAO, SST1 and SST3. Results indicate that the winter NAO is a good predictor for spring SPI values for the northern, central and southern regions of Portugal. On the other hand, the winter SST1 must be considered for the northern region, and the winter SST3 for the southern part.

The aim of this study is twofold: (1) to develop new probabilistic models for short and middle term forecasting of drought transition probabilities, expressed in terms of SPI at different time scales, able to include NAO as exogenous input variable; (2) to quantify the enhancement in forecasting drought transition probabilities with respect to the case when NAO is neglected. In particular, two types of probabilistic models are proposed which result from an analytical derivation of conditional probability of future SPI classes with respect to current SPI (and NAO) classes or current SPI (and NAO) values, under the hypothesis of multivariate normal distribution of the underlying joint variables. Furthermore, a simple score approach to quantitatively assess the corresponding skill in forecasting is applied to identify the best model.

Table 2
Number of transitions between SPI classes at month τ and SPI classes at month $\tau + M$ computed on monthly areal precipitation in Sicily for the period 1922–2008. (Current month τ: February; SPI aggregation time scale $k = 4$ months).

SPI class at month τ	Extreme	Severe	Moderate	Non drought
SPI class at month $\tau + M$ ($M = 1$ month)				
Extreme	0	0	0	0
Severe	0	3	1	3
Moderate	0	2	2	2
Non drought	0	0	3	71
SPI class at month $\tau + M$ ($M = 2$ months)				
Extreme	0	0	0	0
Severe	0	1	2	4
Moderate	0	1	3	2
Non drought	1	0	7	66
SPI class at month $\tau + M$ ($M = 3$ months)				
Extreme	0	0	0	0
Severe	0	0	1	6
Moderate	0	2	1	3
Non drought	2	4	7	61

The main novelty of the proposed methodology is that drought class transition probabilities are expressed in analytical form, with the variance–covariance matrix and the current conditions of the underlying variables as parameters. This feature makes possible to overcome the limitation of alternative approaches, such as frequency analysis of observed transitions in historical samples, or application of Markov chain schemes. This stems from the fact that computation of empirical frequencies can be unreliable due to the generally limited number of transitions observed in historical SPI series, as confirmed by Table 2.

The paper is organized into four sections, besides this introduction. Section 2 describes the study area and data. In Section 3, after a brief description of NAO and SPI, the proposed forecasting models are presented in details. Results are presented and discussed in Section 4, together with a comparison of the models performances by means of a skill score validation technique. Concluding remarks are drawn in Section 5.

2. Study area and data

With a surface area of approximately 25,460 km^2, Sicily is the largest island in the Mediterranean Sea. Its climate is typically Mediterranean, with hot and dry summer seasons and mild and rainy winter seasons, with the only exception of highlands (above 1200 m a.m.s.l.), characterized by fresh summer and cold winter seasons.

About 75% of the total rainfall of the region occurs from October to March, as a result of cyclonic storms. The latter are produced by subtropical high-pressure cells which, during fall/winter season, drift from the northern hemisphere toward the equator, whereas, from May to August, drift back toward the northern hemisphere. Climate features are also highly variable in space due to a rather complex morphology. Indeed, the mountain chain along the northern coast produces higher precipitation and colder temperatures. Southwestern and central areas are predominantly hilly and have the lowest precipitation and highest temperatures in Sicily. The southeastern area is a typical plateau with high temperatures and intermediate precipitation. Mt. Etna (3,300 m a.m.s.l.) exhibits the highest precipitation and the lowest temperature.

Spatial variability of droughts in Sicily region have been investigated by Bonaccorso et al. (2003), based on SPI series computed on monthly precipitation observed in traditional rain gauges and on NCEP/NCAR reanalysis data from 1926 to 1996. Application of Principal Component Analysis on such data has revealed three distinct areas of independent drought variability, namely Northern, Eastern and South-Western Sicily, somehow coincident with the

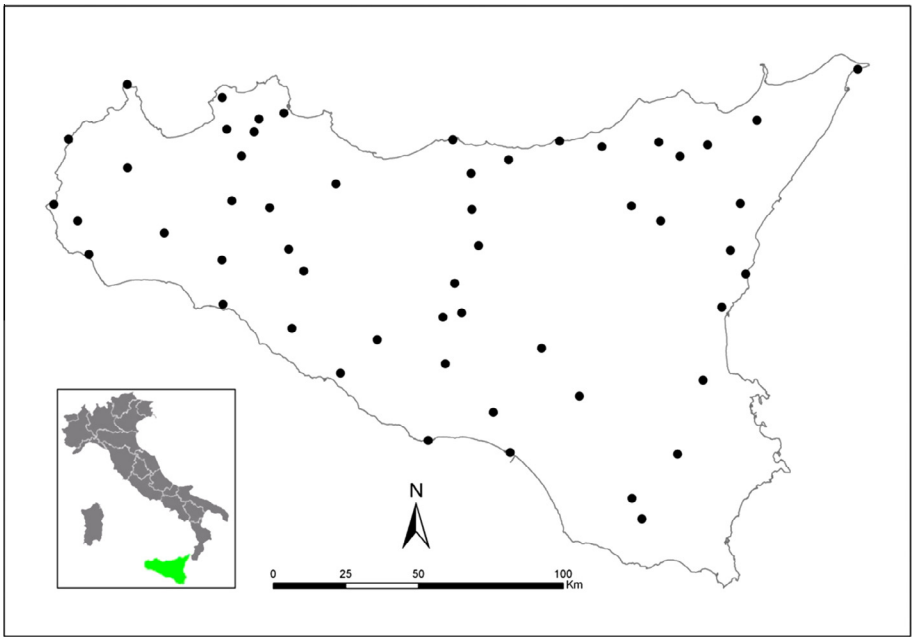

Fig. 1. Study area and location of the 54 rain gauges used for SPI computation.

main climatic sub-regions previously described, thus confirming that different physical causes act on the system.

Di Mauro (2006) has analyzed the influence of ENSO, NAO and EB on rainfall regime in Sicily by means of correlation analysis. With special reference to winter NAO, a significant negative correlation has been observed with mean areal precipitation observed during the past two or three decades. This is in agreement with the fact that during such a period winter NAO has been mostly in a positive phase (Hurrell et al., 2001), meanwhile precipitation in Sicily has been usually below normal values all over the island and mainly in the south-western part. Also, significant negative correlation has been detected between winter NAO and precipitation observed one or even two months ahead, thus suggesting that, in principle, NAO could provide a contribution to drought forecasting.

In the present study, SPI series have been computed on areal monthly precipitation series from 1921 until 2008, obtained by applying the Thiessen polygons method (Thiessen, 1911; Fetter, 1994) on 54 precipitation stations in Sicily (see Fig. 1). The selected stations are operated by the Water Observatory of Sicily Region, formerly the Sicilian Regional Hydrographic Service, whose data are available at www.osservatorioacque.it.

3. Methodology

3.1. The North Atlantic Oscillation index

NAO is the most important pattern of atmospheric circulation variability during the winter season over Europe (Hurrell, 1995; Hurrell et al., 2003). The influence of NAO on European climate, and mainly on precipitation regime, is related to corresponding changes in the associated activity of North-Atlantic storm tracks that affect the western European border (Goodess and Jones, 2002). During the positive phases of NAO, the North Atlantic westerlies, which provide much of the atmospheric moisture to North Africa and Europe, shift northward, giving rise to cold conditions in Northern Europe. This, in turn, results in dry conditions over Southern Europe, the Mediterranean Sea, and Northern Africa. Conversely, the opposite pattern occurs when NAO is in its negative phases (Hurrell and Van Loon, 1997; Trigo et al., 2002; Hurrell et al., 2003).

There are different ways to identify the spatial signature of NAO. As a consequence, there is no universally accepted NAO index to describe the evolution in time of the phenomenon. Readers may refer to Hurrell et al. (2003) for further details. Originally, Walker and Bliss (1932) built the first index based on a linear combination of surface pressure and temperature observations from weather stations on both side of the Atlantic basin. More recently, various NAO indices have been defined by measuring the difference in surface pressure anomalies between various northern and southern sites (station-based indices). Rogers (1984) defined the NAO index by examining the difference in normalized sea level pressure (SLP) between Ponta Delgada (Azores) and Akureyri (Iceland). Recently, researchers have realized that, during the winter season, stations located in Iberian peninsula could be used with some advantages over Ponta Delgada. Hurrell (1995) started to use Lisbon (Portugal) pressure data and Jones et al. (1997) opted for Gibraltar data; also, in both cases Stykkisholmur/Reykjavik (Iceland) was used as location of the northern node. However, it should be stressed that all of these indices are highly correlated, presenting linear correlation coefficient values higher than 0.9.

Station-based NAO indices present some drawbacks. First of all they are fixed in space, therefore they cannot capture the movement of NAO centre of action through the annual cycle. Besides, they may contain noise due to the effect of small scale and transient meteorological phenomena different from NAO. As an alternative, some authors have suggested to apply Principal Component Analysis to sea level pressure (SLP) gridded data to better represent NAO spatial pattern (PC-based indices). Nevertheless, PC-based indices strongly depend on the size of the window used (Trigo et al., 2002), in terms of spatial extent of the grid data. Furthermore, Osborn et al. (1999) have shown that station-based and PC-based NAO indices are very similar in the time evolution, with correlations in the range of 0.84–0.96.

Based on previous considerations, in the present study NAO index computed on the differences between the standardized pressure anomalies measured at Gibraltar and Reykjavik (Iceland), compiled by the Climate Research Unit of the University of East Anglia (UK), was selected for the period 1821–2013 (http://www.cru.uea.ac.uk/cru/data/nao/).

3.2. The Standardized Precipitation Index

The SPI is based on an equi-probability transformation of aggregated monthly precipitation into a standard normal variable. In practice, computation of the index requires: (i) fitting a probability distribution to aggregated monthly precipitation series (e.g. $k = 3, 6, 12, 24$ months, etc.), (ii) computing the non-exceedance probability of such aggregated value and (iii) defining the corresponding standard normal quantile as the SPI. McKee et al. (1993) assumed aggregated precipitation series as gamma distributed and used a maximum likelihood method to estimate the parameters of the distribution.

The SPI index is able to take into account the different time scales at which the drought phenomenon occurs and, because of its standardization, is particularly suited to compare drought conditions among different time periods and regions with different climatic conditions (Hayes et al., 1999; Bonaccorso et al., 2003).

By virtue of such relevant strengths, SPI has achieved a lot of popularity for drought monitoring purposes all over the world. Indeed, the Sixteenth World Meteorological Congress, organized by the World Meteorological Organization, adopted Resolution 21 (Cg-XVI) on the "Use of the standardized precipitation index for characterizing meteorological droughts by all National Meteorological and Hydrological Services" (WMO, 2011).

Nevertheless, SPI has a main weakness. Since SPI is a precipitation-based drought index, it relies on the assumption that precipitation has a stronger influence on drought phenomena than any other variables, such as temperature and potential evapotranspiration (PET). This is a valid assumption in case that temporal variability in precipitation is larger than temperature fluctuations. Therefore, application of drought indices including temperature data (such as the PDSI or SPEI) is recommended, for instance, in climate change impact studies involving future scenarios or when positive trend observed in long term temperature series are more significant than negative trend detected in precipitation series, as is the case of Italy (Brunetti et al., 2006).

In spite of previous considerations, it should be pointed out that the focus of the study is not on drought analysis in the context of global warming, but rather on developing and testing new drought forecasting models able to take into account exogenous variables, such as large scale atmospheric circulation patterns. To this end, investigating the appropriateness of the SPI vs. any other standardized indices (as well as of NAO vs. other exogenous variables) is beyond the scope of the paper. Furthermore, the probabilistic structure of the proposed models is flexible enough to be applied to any other standardized drought monitoring indices, such as SPEI.

Although McKee et al. (1993) originally proposed a classification restricted to dry conditions, it has become customary to use SPI to classify also wet periods. Table 3 reports the SPI climatic classification provided by the National Drought Mitigation Center (NDMC, http://drought.unl.edu). Also, the probabilities ΔP, that the index lies within each class are listed. Since the present work focuses on forecasting drought conditions, in what follows the near normal and wet classes have been grouped into one class termed "Non-drought".

In the present study, SPI series have been computed on monthly precipitation aggregated at three different time scales k. In particular, short to medium aggregation time scales, namely $k = 3, 4, 6$ months (i.e. SPI-3, SPI-4 and SPI-6), have been selected in order to better capitalize on the potential contribution of NAO to the predictive skill of the proposed models.

3.3. SPI Drought transition probabilities

3.3.1. Transition probabilities from a current SPI drought class to a future drought class

Transition probabilities between SPI-based drought classes can be expressed in terms of conditional probability that SPI lies within a drought class at the future month $\tau + M$, given the SPI drought class at the current month τ, for every month τ and time horizon M.

Let $Z_{v,\tau}$ be the SPI value at year v and month $\tau = 1, 2, \ldots, 12$, for a given aggregation time scale of monthly precipitation. Also, let C_i be the generic drought class, for instance C_1 = Extreme, C_2 = Severe, C_3 = Moderate, C_4 = Non-drought. The probability that the SPI value after M months lies within a class C_M, with class limits (C_{Mi} and C_{Ms}), given that the SPI value at the current month lies within a class C_0, with class limits (C_{0i} and C_{0s}), can be expressed, by definition of conditional probability, as:

$$P[Z_{v,\tau+M} \in C_M | Z_{v,\tau} \in C_0] = \frac{\int_{C_{M_i}}^{C_{M_s}} \int_{C_{0_i}}^{C_{0_s}} f_{Z_{v,\tau}, Z_{v,\tau+M}}(t,s) \cdot \mathrm{d}t \cdot \mathrm{d}s}{\int_{C_{0_i}}^{C_{0_s}} f_{Z_{v,\tau}}(t) \cdot \mathrm{d}t} \quad (1)$$

where $f_{Z_{v,\tau}, Z_{v,\tau+M}}(\cdot)$ is the joint density function of $Z_{v,\tau}$ and $Z_{v,\tau+M}$, $f_{Z_{v,\tau}}(\cdot)$ is the marginal density function of $Z_{v,\tau}$, t and s are integration dummy variables, C_{Mi} and C_{Ms} are the lower and the upper bounds of the future drought class C_M, while C_{0i} and C_{0s} are the lower and the upper bounds of the current drought class C_0.

Since, by definition, SPI is marginally distributed as a standard normal variable, it is fair to assume, without loss of generality, the joint density function in Eq. (1) to be bivariate normal (Cancelliere et al., 2007). Such an assumption is not limiting since other multivariate distributions could be assumed in what follows, for instance based on copulas, according to the particular investigated area.

Thus, the computation of transition probabilities in Eq. (1) requires the determination of the autocovariance at lag M of $\boldsymbol{Z}_{v,\tau+M}$, namely $cov[Z_{v,\tau}, Z_{v,\tau+M}]$. Such autocovariance can be estimated by computing the sample counterpart from the SPI series under investigation. Alternatively, the autocovariance of $\boldsymbol{Z}_{v,\tau+M}$ can be derived, under the hypothesis of uncorrelated and normally distributed monthly precipitation aggregated at various time scales k, as a function of the statistics of the underlying precipitation (Cancelliere et al., 2007). In what follows, the former approach has been applied.

Table 3
Wet and drought period classification according to the SPI.

SPI values	Class	Probability	ΔP	
$\geqslant 2.00$	Extremely wet	0.977–1.000	0.023	Non drought (N)
1.50–1.99	Very wet	0.933–0.977	0.044	
1.00–1.49	Moderately wet	0.841–0.933	0.092	
−0.99 to 0.99	Near normal	0.159–0.841	0.682	
−1.49 to −1.00	Moderate drought (Mo)	0.067–0.159	0.092	
−1.99 to −1.50	Severe drought (Se)	0.023–0.067	0.044	
$\leqslant -2.00$	Extreme drought (Ex)	0.000–0.023	0.023	

The above computation of the transition probabilities can be extended by including an exogenous variable in the model. Considering another variable $W_{v,\tau}$ (e.g. NAO) with its respective class limits (C_{wi} and C_{ws}), the conditional probability given by Eq. (1) becomes:

$$P[Z_{v,\tau+M} \in C_M | Z_{v,\tau} \in C_o, W_{v,\tau} \in C_w] = \frac{\int_{C_{M_i}}^{C_{M_s}} \int_{C_{o_i}}^{C_{o_s}} \int_{C_{w_i}}^{C_{w_s}} f_{Z_{v,\tau+M},Z_{v,\tau},W_{v,\tau}}(t,s,w) \cdot dt \cdot ds \cdot dw}{\int_{C_{o_i}}^{C_{o_s}} \int_{C_{w_i}}^{C_{w_s}} f_{Z_{v,\tau},W_{v,\tau}}(s,w) \cdot ds \cdot dw} \quad (2)$$

Again, without loss of generality, assuming the joint distribution of the three-dimensional random vector $\mathbf{X} = [Z_{v,\tau+M}, Z_{v,\tau}, W_{v,\tau}]$ as multivariate normal, the probability density at the numerator is given by:

$$f_{Z_{v,\tau+M},Z_{v,\tau},W_{v,\tau}}(t,s,w) = \frac{1}{(2\pi)^{3/2}|\Sigma|^{1/2}} \cdot \exp\left(-\frac{1}{2}\mathbf{x}^T\Sigma^{-1}\mathbf{x}\right) \quad (3)$$

where $\mathbf{x} = [t,s,w]$ and $\sum$ is the variance–covariance matrix:

$$\Sigma = \begin{bmatrix} 1 & cov[Z_{v,\tau+M}, Z_{v,\tau}] & cov[Z_{v,\tau+M}, W_{v,\tau}] \\ cov[Z_{v,\tau}, Z_{v,\tau+M}] & 1 & cov[Z_{v,\tau}, W_{v,\tau}] \\ cov[W_{v,\tau}, Z_{v,\tau+M}] & cov[W_{v,\tau}, Z_{v,\tau}] & var[W_{v,\tau}] \end{bmatrix} \quad (4)$$

since $\text{var}[Z_{v,\tau}] = \text{var}[Z_{v,\tau+M}] = 1$. Let $\mathbf{X}_1 = [Z_{v,\tau}, W_{v,\tau}]$, then the bivariate density at the denominator is:

$$f_{Z_{v,\tau},W_{v,\tau}}(s,w) = \frac{1}{2\pi|\Sigma_1|^{1/2}} \cdot \exp\left(-\frac{1}{2}\mathbf{x}_1^T\Sigma_1^{-1}\mathbf{x}_1\right) \quad (5)$$

where $\mathbf{x}_1 = [s,w]$ and $\sum_1$ is the variance–covariance matrix:

$$\Sigma_1 = \begin{bmatrix} 1 & cov[Z_{v,\tau}, W_{v,\tau}] \\ cov[Z_{v,\tau}, W_{v,\tau}] & var[W_{v,\tau}] \end{bmatrix} \quad (6)$$

Integration of the triple and double integral of Eq. (2) can be carried out numerically, for instance by means of the algorithm MULNOR (Schervish, 1984).

In order to investigate the potential of NAO index as exogenous variable within the proposed model, results from the application of Eqs. (1) and (2) must be compared. First, a classification of NAO index phases is required. Some authors (e.g. Gimeno et al., 2002; Muñoz-Diaz and Rodrigo, 2004; Lopez-Moreno et al., 2007) adopted a three phases classification, based on mean plus or minus standard deviation bounds. Here, given the significant negative correlation observed between NAO and SPI series, a symmetrical classification with respect to the one adopted for SPI has been chosen. In particular, four classes have been considered with limits C_{wi} and C_{ws} in Eq. (2): $]-\infty, 1[$, $[1, 1.5[$, $[1.5, 2[$, $[2, +\infty[$. Despite such classification is rather arbitrary, it should be pointed out that our interest lies in verifying the influence of NAO rather than in selecting a proper classification. Nonetheless, it may be worthwhile to note that the use of other classifications have been also explored yielding similar results, at least from a qualitative point of view.

Furthermore, an analysis oriented to assess whether differences in transition probabilities are due to sampling variability or to an effective influence of NAO on SPI values in Sicily is carried out. To this end, confidence intervals are derived by generating from a normal distribution 100 NAO series uncorrelated with the observed SPI series, and by computing, for each considered transition, the corresponding 100 transition probabilities by Eq. (2). Confidence limits at 10% significance level are then estimated by considering the lower and upper 5% quantiles of such transition probabilities. Thus, if transition probabilities computed on observed series lie outside the confidence intervals, the null hypothesis of uncorrelated series is rejected and therefore NAO must be considered to have a significant influence on SPI drought transitions in Sicily.

3.3.2. Transition probabilities from a current SPI value to a future drought class

Transition probabilities between drought conditions can also be determined by conditioning on current SPI value. The rationale of this approach is that transitions probabilities are rather to be affected by the particular value currently taken by SPI than by the corresponding class. For instance, transition toward Non drought class ($\text{SPI} \geqslant -1$) from a moderate class ($-1.5 < \text{SPI} < -1$) should be more or less probable, depending whether the observed SPI is closer to the class upper bound or to the class lower bound. More specifically, the interest lies in computing $P[Z_{v,\tau+M} \in C_M | Z_{v,\tau} = z_0]$, namely the transition probability toward the SPI class C_M at month $\tau + M$, given SPI value z_0 at month τ.

Once again, the SPI variables $Z_{v,\tau}$ and $Z_{v,\tau+M}$ are assumed to be joint normal distributed with zero mean and variance equal to one. Then, according to a well known statistical property of multivariate normal distributions, the conditional distribution of $Z_{v,\tau+M}|Z_{v,\tau} = z_0$ will be normal, with mean and variance (Mood et al., 1988):

$$E[Z_{v,\tau+M}|Z_{v,\tau}] = \mu_{Z_{v,\tau+M}} + (\rho \cdot \sigma_{z_{v,\tau+M}}/\sigma_{z_{v,\tau}}) \cdot (z_0 - \mu_{Z_{v,\tau}}) = \rho \cdot z_0 \quad (7)$$

$$var[Z_{v,\tau+M}|Z_{v,\tau}] = \sigma^2_{Z_{v,\tau+M}}(1-\rho^2) = 1-\rho^2 \quad (8)$$

where ρ is the linear correlation coefficient between SPI series at the present month τ and at month $\tau + M$.

It follows that the transition probability from the current SPI value z_0 at month τ to a future drought class C_M will be given by:

$$P[Z_{v,\tau+M} \in C_M | Z_{v,\tau} = z_0] = \int_{C_{Mi}}^{C_{Ms}} \frac{1}{\sqrt{2\pi}\sigma_Z} \cdot e^{-\frac{1}{2}\left(\frac{x-\rho \cdot z_0}{1-\rho^2}\right)^2} dx = \Phi\left[\frac{C_{Ms} - \rho \cdot z_0}{1-\rho^2}\right] - \Phi\left[\frac{C_{Mi} - \rho \cdot z_0}{1-\rho^2}\right] \quad (9)$$

where in usual notation Φ represents the standard normal cdf and x is the integration dummy variable.

The previous methodology can be extended in order to condition also on an exogenous variable. More specifically, with reference to another variable $W_{v,\tau}$, the probability of interest will be:

$$P[Z_{v,\tau+M} \in C_M | Z_{v,\tau} = z_0, W_{v,\tau} = w_0] \quad (10)$$

Assuming the joint distribution of $Z_{v,\tau+M}, Z_{v,\tau}, W_{v,\tau}$ as multivariate normal, the distribution of $Z_{v,\tau+M}$ conditioned on $Z_{v,\tau}, W_{v,\tau}$ will be normal with mean and variance:

$$E[Z_{v,\tau+M}|Z_{v,\tau}, W_{v,\tau}] = \mu_z = \sum_{12} \cdot \sum_{22}^{-1} \cdot \begin{bmatrix} z_0 \\ w_0 \end{bmatrix} \quad (11)$$

$$\text{var}[Z_{v,\tau+M}|Z_{v,\tau}, W_{v,\tau}] = \sigma_z^2 = 1 - \sum_{12} \cdot \sum_{22}^{-1} \cdot \sum_{21} \quad (12)$$

where

$$\sum_{12} = [cov(Z_{v,\tau+M}, Z_{v,\tau}) \quad cov(Z_{v,\tau+M}, W_{v,\tau})] \quad (13)$$

$$\sum_{22} = \begin{bmatrix} 1 & cov[Z_{v,\tau}, W_{v,\tau}] \\ cov[W_{v,\tau}, Z_{v,\tau}] & 1 \end{bmatrix} \quad (14)$$

$$\sum_{21} = \sum_{12}^T \quad (15)$$

Then, Eq. (10) will become:

$$P[Z_{v,\tau+M} \in C_M | Z_{v,\tau} = z_0, W_{v,\tau} = w_0] = \int_{C_{Mi}}^{C_{Ms}} \frac{1}{\sqrt{2\pi}\sigma_Z} \cdot e^{-\frac{1}{2}\left(\frac{x-\mu_Z}{\sigma_Z}\right)^2} dx \quad (16)$$

4. Results and discussion

4.1. Correlation analysis

A preliminary correlation analysis between SPI series in Sicily and NAO index series has been carried out by means of linear correlation coefficient. The choice of such correlation coefficient is justified by the fact that SPI series are normally distributed by definition and that NAO series can be considered normally distributed as well (Muñoz-Diaz and Rodrigo, 2004; Lopez-Moreno and Vicente-Serrano, 2008).

Previous studies (Di Mauro, 2006) indicate that the correlation between NAO and SPI in Sicily appears stronger when recent decades are considered. Thus, the last three decades of available data (1979–2008) have been selected here as investigated period, so as to have a sufficiently long dataset. SPI sample series, as well as NAO series, have been preliminarily standardized in order to preserve the zero mean and unit variance. NAO series have been averaged on a period of 3, 4 and 6 months, ending either in the same month as SPI, or 1 month, 2 months and 3 months before, for each month of the year.

In Fig. 2 correlation coefficients between NAO series and SPI series are shown in grey color scale for different combinations of SPI aggregation time scale k (rows) and NAO average period (AP) (columns), for each month (x-axis) and for the different lead time M of SPI with respect to NAO (0, 1, 2, 3 months – y-axis).

The plots highlight that higher negative correlations (with values generally less than −0.5) between NAO and SPI series are generally observed from February to April for almost all the considered cases. Furthermore from the plots, it can be inferred that NAO averaged on a period of 4 or 6 months lead to higher correlation coefficients in most cases.

In addition, Table 4 shows correlation values between NAO (average period AP: 4 months, ending respectively in January, February, March and April), and SPI series (k = 3, 4 and 6 months), for lead time M = 0, 1, 2 and 3 months. Numbers in bold indicate values of correlation for which the null hypothesis of uncorrelated variables is rejected according to the T test (Helsel and Hirsh, 1992) at 5% significance level. From the table it can be inferred that the null hypothesis is rejected for almost all values. Moreover, the highest values of correlation correspond to NAO series averaged on the period from November to February or from December to March.

The results of such preliminary correlation analysis are in general agreement with findings of previous studies focusing on Europe and the Mediterranean region (Hurrell, 1995; Cullen and deMenocal, 2000; Lopez-Moreno and Vicente-Serrano, 2008; Brandimarte et al., 2011; Ferrari et al., 2013).

On the basis of the results of the correlation analysis, an average period of 4 months has been considered for NAO index in the following applications.

In addition, NAO and SPI samples corresponding to different combinations of k, M and AP have been tested for multivariate normality by means of the Mardia test (Mardia, 1970). Results, here not shown for the sake of brevity, reveal that in most cases the assumption of multivariate normality cannot be rejected at 5% significance level.

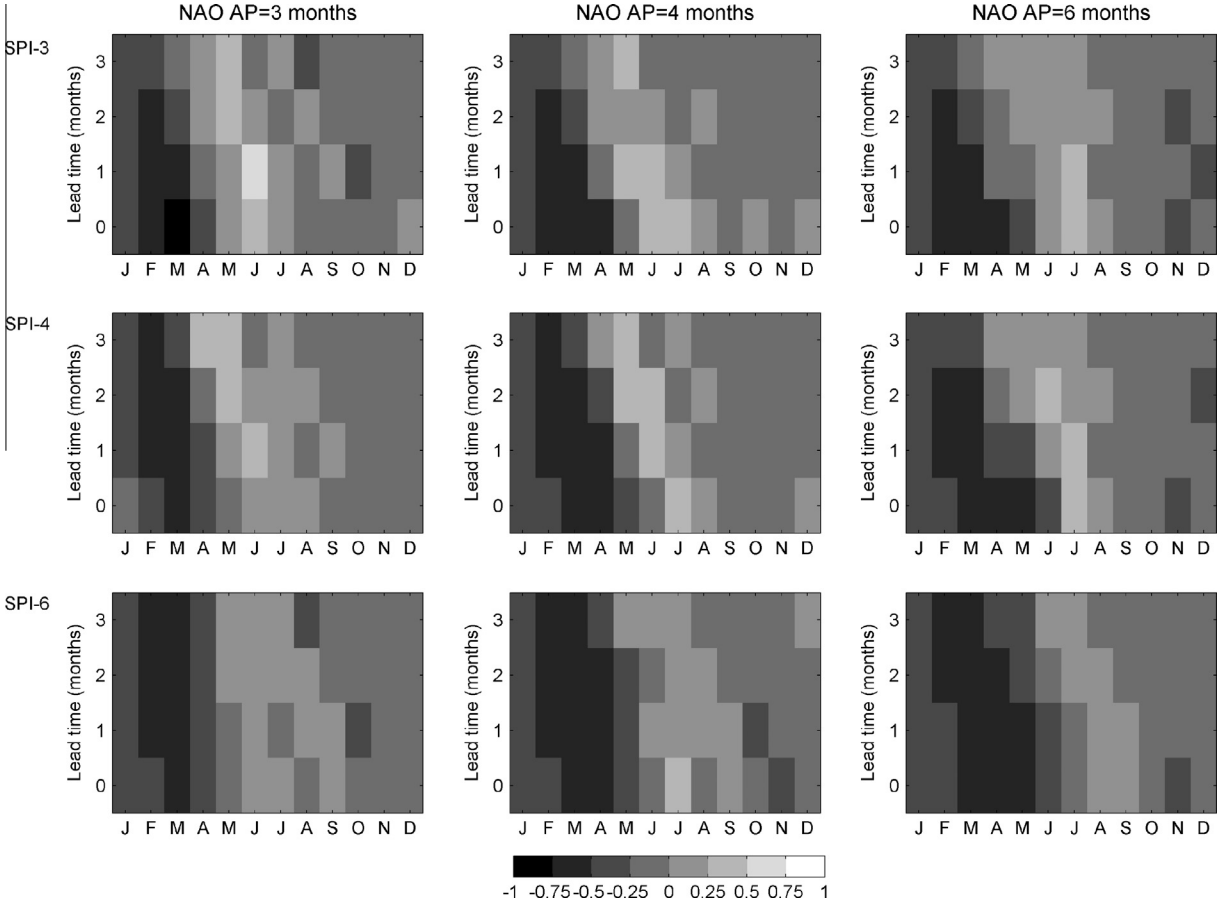

Fig. 2. Linear correlation coefficients between NAO series (average period AP = 3, 4, 6 months) and SPI series (time aggregation scale k = 3, 4, 6 months), for each month and for different lead times (M = 0, 1, 2, 3 months).

Table 4
Correlation coefficient between NAO (averaging period *AP*: 4 months) and SPI series (aggregation time scale *k*: 3, 4, 6 months), for lead time 0, 1, 2 and 3 months. Bold types indicate significant correlation values (α = 5% significance level).

SPI aggregation time scale *k*	Ending month of NAO average period	SPI lead time *M*			
		0 months	1 month	2 months	3 months
3 months	January	−0.320	**−0.447**	**−0.361**	**−0.367**
	February	**−0.558**	**−0.638**	**−0.573**	−0.277
	March	**−0.691**	**−0.631**	**−0.364**	−0.180
	April	**−0.592**	−0.238	0.054	0.121
4 months	January	−0.269	**−0.385**	**−0.430**	**−0.482**
	February	**−0.490**	**−0.629**	**−0.661**	**−0.514**
	March	**−0.682**	**−0.687**	**−0.605**	**−0.375**
	April	**−0.663**	**−0.513**	−0.253	0.094
6 months	January	−0.320	−0.356	**−0.362**	**−0.453**
	February	**−0.427**	**−0.540**	**−0.565**	**−0.591**
	March	**−0.613**	**−0.602**	**−0.649**	**−0.650**
	April	**−0.612**	**−0.548**	**−0.590**	**−0.464**

4.2. Transition probabilities from current SPI drought class to future class

Several combination of NAO average period *AP*, SPI aggregation time scale *k* and forecasting horizon *M* have been considered. For the sake of brevity, here only few significant cases are presented. In particular, transition probabilities of SPI-4 and SPI-6 drought classes, considering February or March as current month τ, NAO *AP* = 4 months and *M* = 1, 2, 3 months as forecasting horizon, are reported hereinafter.

In Fig. 3 transition probabilities of SPI-4 drought classes from February to April (i.e. *M* = 2) are shown. For each transition probability values are depicted by bars. In particular, black bars correspond to transition probabilities computed by Eq. (1), namely regardless of NAO current class. On the other hand, transition probabilities computed by Eq. (2) are represented by different colored bars (from white to dark grey), according to the current NAO class. The lower and upper 5% quantiles of generated transition probabilities, under the hypothesis of uncorrelated NAO and SPI series, are indicated by black crosses.

From the inspection of the figure some interesting considerations can be drawn. First, when transitions related to persisting or worsening drought conditions (e.g. Ex/Ex, Se/Ex, Se/Se, etc.) are considered, the corresponding probabilities significantly increase as NAO index tends toward extremely positive values (i.e. NAO > 2). On the other hand, considering drought conditions that turn to a less severe or to a Non drought class (e.g. Ex/Se, Ex/Mo, Se/Mo, Ex/N, etc.) leads to transition probabilities that decrease as NAO value increases.

Moreover, it can be observed that transitions probabilities are generally outside the confidence intervals (i.e. 50 cases out of 64) computed under the hypothesis of uncorrelated NAO and SPI series, which indicates that NAO series, averaged on the period November–February, could exert a significant influence on drought class transitions in April. For instance, transition probabilities from Non-drought toward all classes (Fig. 3d) are outside the confidence intervals. In other cases however, some probabilities lie within the confidence intervals and therefore the influence of NAO does not appear significant.

Similar considerations can be clearly drawn for *M* = 1, that is for drought class transition probabilities from February to March. When considering drought class transition probabilities of SPI-4 from February to May (i.e. *M* = 3), the hypothesis of uncorrelated series is still rejected for a significant number of cases, e.g. 44 out of 64.

On equal aggregation time scale (*k* = 4 months) and NAO series averaged on the period December–March, the number of transitions probabilities outside the confidence intervals decreases to 32 for *M* = 2 (i.e. drought class transition from March to May) and to 8 out of 64 for *M* = 3 (i.e. drought class transition from March to June), suggesting a minor contribution of NAO series in forecasting SPI-4 drought class transitions probabilities.

On the other hand, a major influence of NAO on SPI series is observed when a longer aggregation time scale is considered, as it can be inferred from Fig. 4 where transition probabilities of SPI-6 drought classes from March to June (i.e. *M* = 3) are shown.

Previous considerations are confirmed by Tables 5 and 6 where the most probable transition classes of SPI-4 and SPI-6, respectively, are reported for all the considered NAO classes (Eq. (2)) and compared to the ones obtained when NAO index is neglected (Eq. (1)). Results show that, while Non drought condition (N) is usually the most probable future class when NAO is not considered (with the exception of Extreme (Ex) drought as current SPI class which is likely to remain Extreme 1 month ahead for *k* = 4 months and for every considered *M* for *k* = 6 months, and Severe (Se) which is likely to turn into Moderate (Mo) 1 month ahead for *k* = 4 and 6 months), different outcomes are generally obtained when the effect of NAO is included in the model.

In particular, for *k* = 4 and *M* = 1, assuming Severe and Moderate drought as current SPI classes, NAO < 1.5 leads to less severe drought classes in the future, 1.5 ⩽ NAO < 2 leads to the same drought classes, while NAO ⩾ 2 leads to worse drought conditions. Similar results are obtained for *k* = 6 and *M* = 2 months, at least when the current class is Severe. For *M* = 3 months, the influence of NAO is generally restricted to the cases of NAO > 2, for *k* = 4 and NAO > 1.5 for *k* = 6.

It is worth underlying that, for all the considered cases, a current Non drought condition tends toward a Non drought condition in the future regardless of the particular NAO value. This apparent inertia can be mainly explained by reminding that, according to the adopted terminology, a Non drought condition also include wet conditions.

4.3. Transition probabilities from a current spi value to a drought class

Transition probabilities from SPI and NAO values at current month τ to a drought class in a future month $\tau + M$ have been determined based on Eq. (16) and compared to the ones obtained by Eq. (9), where current NAO value is neglected. Figs. 5 and 6 illustrate in grey color scale transition probabilities to future drought classes (Ex, Se, Mo, N in columns), one month, two months and three months ahead (rows). In the figures February and March has been assumed as current month, *k* = 4 and 6 months as aggregation time scale for SPI values z_0 (i.e. SPI-4 and SPI-6) and

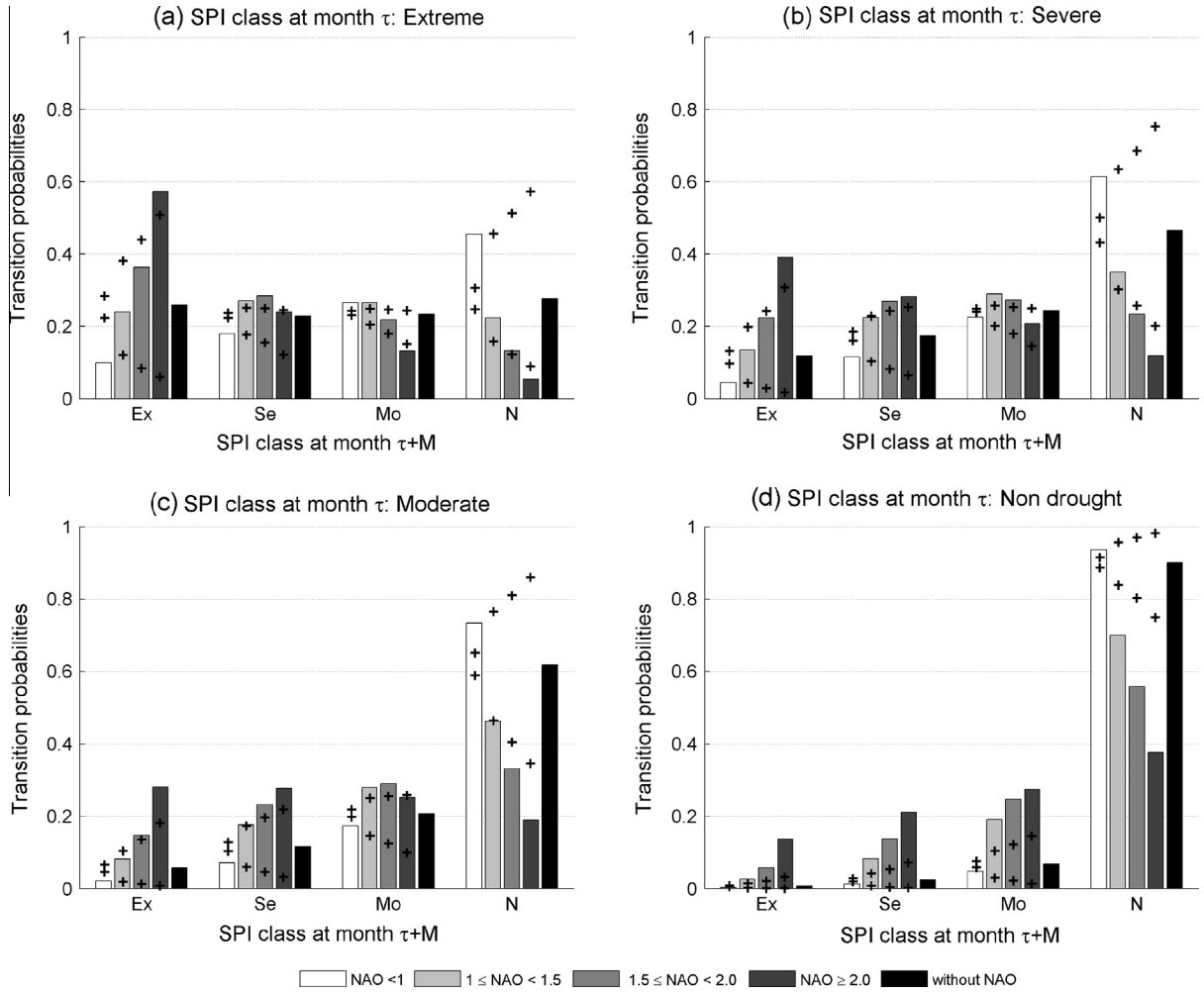

Fig. 3. Transition probabilities of SPI-4 drought classes from February to April (i.e. $M = 2$), for different SPI class at current month τ: (a) Extreme (Ex), (b) Severe (Se), (c) Moderate (Mo), and (d) Non-drought (N). NAO $AP = 4$ months. Transition probabilities are depicted as colored bars, while lower and upper 5% quantiles of generated transition probabilities, under the hypothesis of uncorrelated NAO and SPI series, are indicated by black crosses.

$AP = 4$ months as average period for NAO values w_0, that is from November to February (in Fig. 5) and from December to March (in Fig. 6).

For each considered transition and time horizon M two plots are depicted: transition probabilities considering current SPI values z_0 (x-axis) and NAO values w_0 (y-axis) are shown in the larger images; transition probabilities considering only current SPI values z_0 are shown in the smaller images. For a better representation, only the portion of the plots corresponding to negative values of current SPI is depicted.

From the figures it can be inferred that transition probabilities vary significantly when different SPI or NAO current values are taken into account. For instance, with reference to the top left larger image in Fig. 5 ($k = 4$, $M = 1$, future class extreme), it can be inferred that for values of the current SPI z_0 close to -3, transition probabilities range from 0–0.2 to 0.8–1 as NAO values w_0 increase. Meanwhile, when NAO values are not taken into account (top left smaller image), transition probabilities are always between 0.6 and 0.8. Similar considerations can be drawn with reference to the other cases.

It may be worthwhile to note that the slope of the stripes in the z_0 vs. w_0 larger images can be interpreted as a measure of the relative influence of NAO value w_0 on transition probabilities, compared to the influence of the current SPI value z_0. In particular, it can be expected that the stripes would be perfectly vertical if transition probabilities were only functions of the current SPI value. Conversely, they should be perfectly horizontal if the effect of NAO on transition to a future drought class would be exclusive or, in other words, if current SPI values had no influence on transitions to future values. To this end, one can observe a stronger influence of NAO averaged from November to February on SPI-4, than the one exerted by NAO averaged from December to March on SPI-6, as suggested by previous results of transition probabilities from class to class (see Section 4.2).

For transition to an extreme drought condition, probability values increases as NAO value w_0 increases and SPI value z_0 decreases. In particular, the highest values of transition probabilities generally correspond to extreme drought as starting class. Thus, if an extreme drought is ongoing and positive NAO values are observed, such a drought condition is likely to overstay in the next M months.

Conversely, transition probabilities to Non Drought conditions increase as NAO value w_0 decreases and SPI value z_0 increases. On the other hand, transition probabilities to Severe and Moderate classes present a different pattern, namely probability values first increase and then decrease as NAO value w_0 increases and SPI value z_0 decreases. In particular, high values of transition probabilities from a current drought class to a less severe drought condition correspond to negative NAO values, while the probability to overstay in the same drought class or to move to a worse drought class

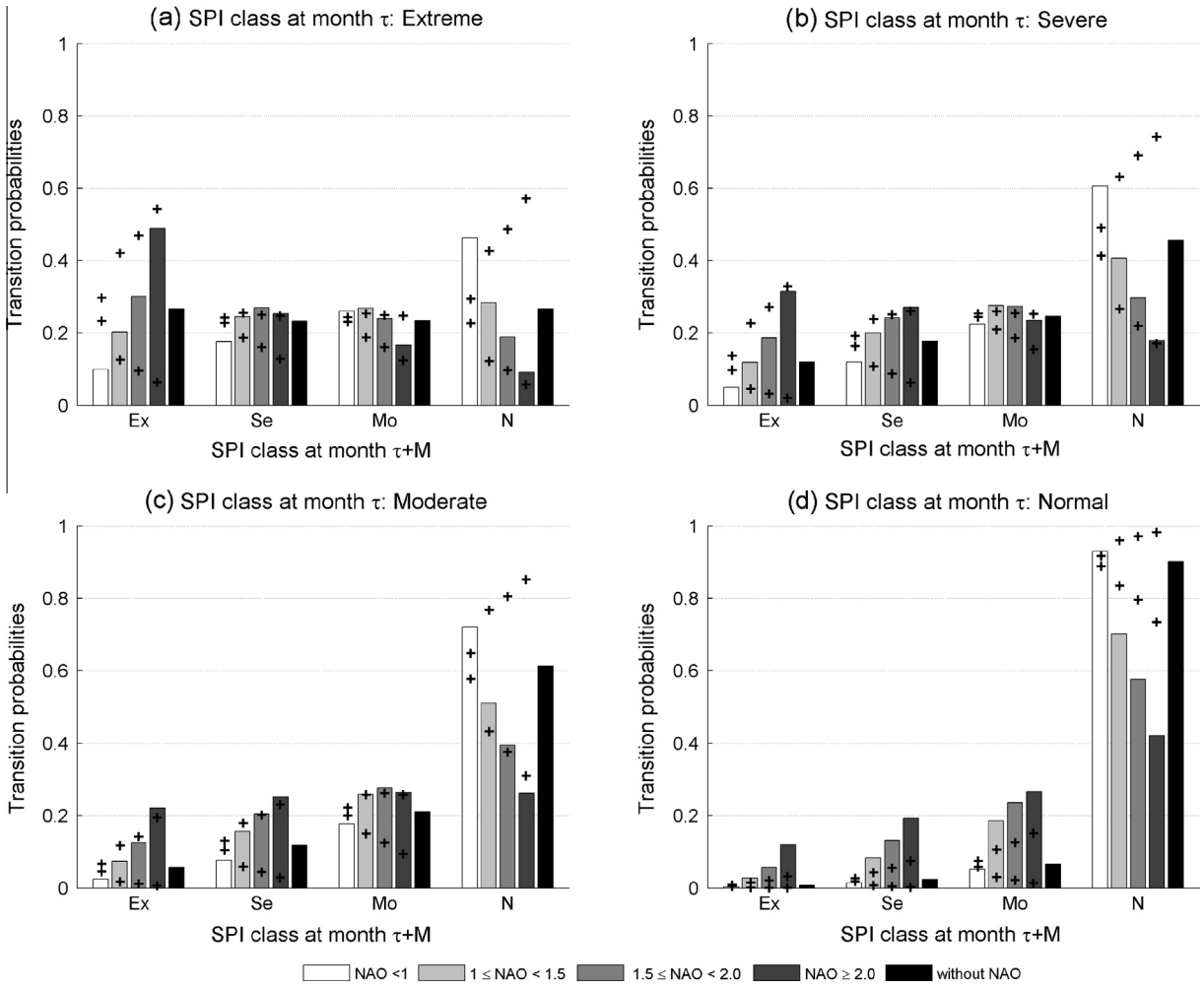

Fig. 4. As in Fig. 3 but for transition probabilities of SPI-6 drought classes from March to June (i.e. $M = 3$).

Table 5
Most probable SPI-4 transition classes either with and without taking into account NAO index, for different time horizon M (current month τ: February).

SPI-4					
SPI class at February	NAO $[-\infty, 1]$	NAO [1, 1.5]	NAO [1.5, 2]	NAO $[2, +\infty]$	Without NAO
SPI class at March (M = 1 month)					
Ex	Se	Ex	Ex	Ex	Ex
Se	N	Mo	Se	Ex	Mo
Mo	N	N	Mo	Se	N
N	N	N	N	N	N
SPI class at April (M = 2 months)					
Ex	N	Se	Ex	Ex	N
Se	N	N	Mo	Ex	N
Mo	N	N	N	Ex	N
N	N	N	N	N	N
SPI at May (M = 3 months)					
Ex	N	N	N	Ex	N
Se	N	N	N	N	N
Mo	N	N	N	N	N
N	N	N	N	N	N

M months ahead increases as NAO value w_0 tends toward extremely positive values.

Furthermore, the time horizon M appears to have an influence on the slope of the stripes. More specifically, while for the case $M = 1$ month the effect of SPI values z_0 on transition probabilities looks predominant over NAO values, the influence of the latter prevails on the former as the forecasting time horizon M increases.

As an example, in order to better quantify the relative influence of SPI and NAO values on drought class transitions, probability values of transition from current SPI-4 values at February to an extreme drought class M months ahead, computed both by Eqs.

Table 6
Most probable SPI-6 transition classes either with and without taking into account NAO index, for different time horizon M (current month τ: March).

SPI-6					
SPI class at March	NAO $[-\infty, 1]$	NAO [1, 1.5]	NAO [1.5, 2]	NAO $[2, +\infty]$	Without NAO
SPI at April (M = 1 month)					
Ex	Ex	Ex	Ex	Ex	Ex
Se	Mo	Se	Se	Se	Mo
Mo	N	N	Mo	Mo	N
N	N	N	N	N	N
SPI at May (M = 2 months)					
Ex	Mo	Ex	Ex	Ex	Ex
Se	N	Mo	Se	Ex	N
Mo	N	N	N	Mo	N
N	N	N	N	N	N
SPI at June (M = 3 months)					
Ex	N	N	Ex	Ex	Ex
Se	N	N	N	Ex	N
Mo	N	N	N	Mo	N
N	N	N	N	N	N

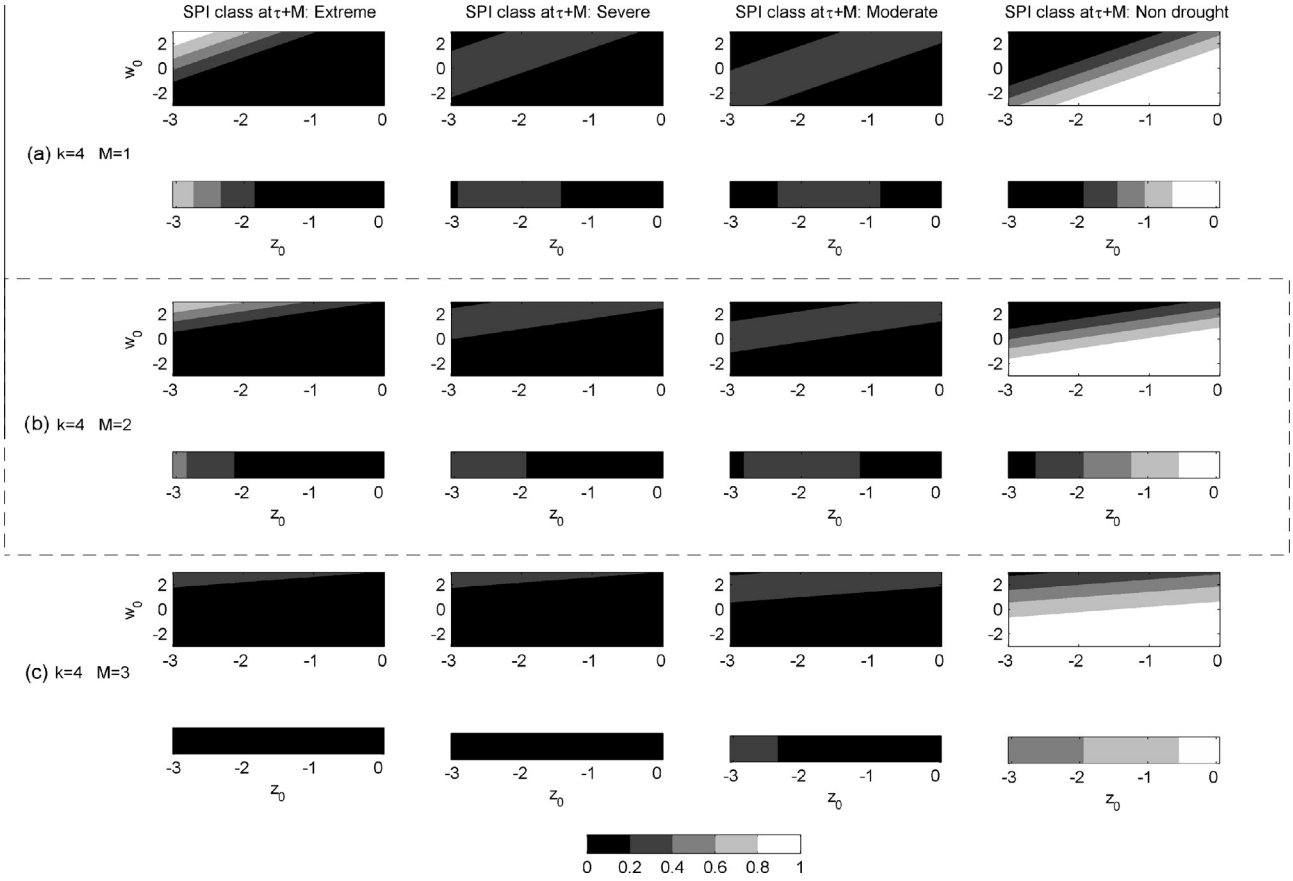

Fig. 5. Transition probabilities to future SPI-4 drought classes for different time horizon M considering either current SPI z_0 and NAO w_0 values (larger images) or only current SPI z_0 values (smaller images) (current month τ: February, NAO AP = 4 months).

(9) and (16), are reported in Table 7. Results confirm that transition probabilities related to a fixed SPI value z_0 change significantly according to the current NAO value.

Finally, Fig. 7 shows the most probable SPI-4 and SPI-6 future classes of transition, either with (larger images) or without (smaller images) taking into account current values of NAO index, for all the considered time horizon M. The first six plots from the top refer to SPI-4 and NAO values w_0 averaged on the period from November to February (i.e. February as current month), while the last six refer to SPI-6 and NAO values w_0 averaged on the period from December to March (i.e. March as current month).

As it can be observed, the most probable future class can vary significantly when different SPI or NAO current values are considered. In particular, worse drought conditions are more likely to occur for fixed SPI value z_0 as NAO value w_0 increases. For instance, for z_0 equal to -2 the most probable class varies from Non drought (N), for lower values of w_0, to Extreme (Ex), for extremely positive values of w_0. Conversely, if NAO values are not taken into account

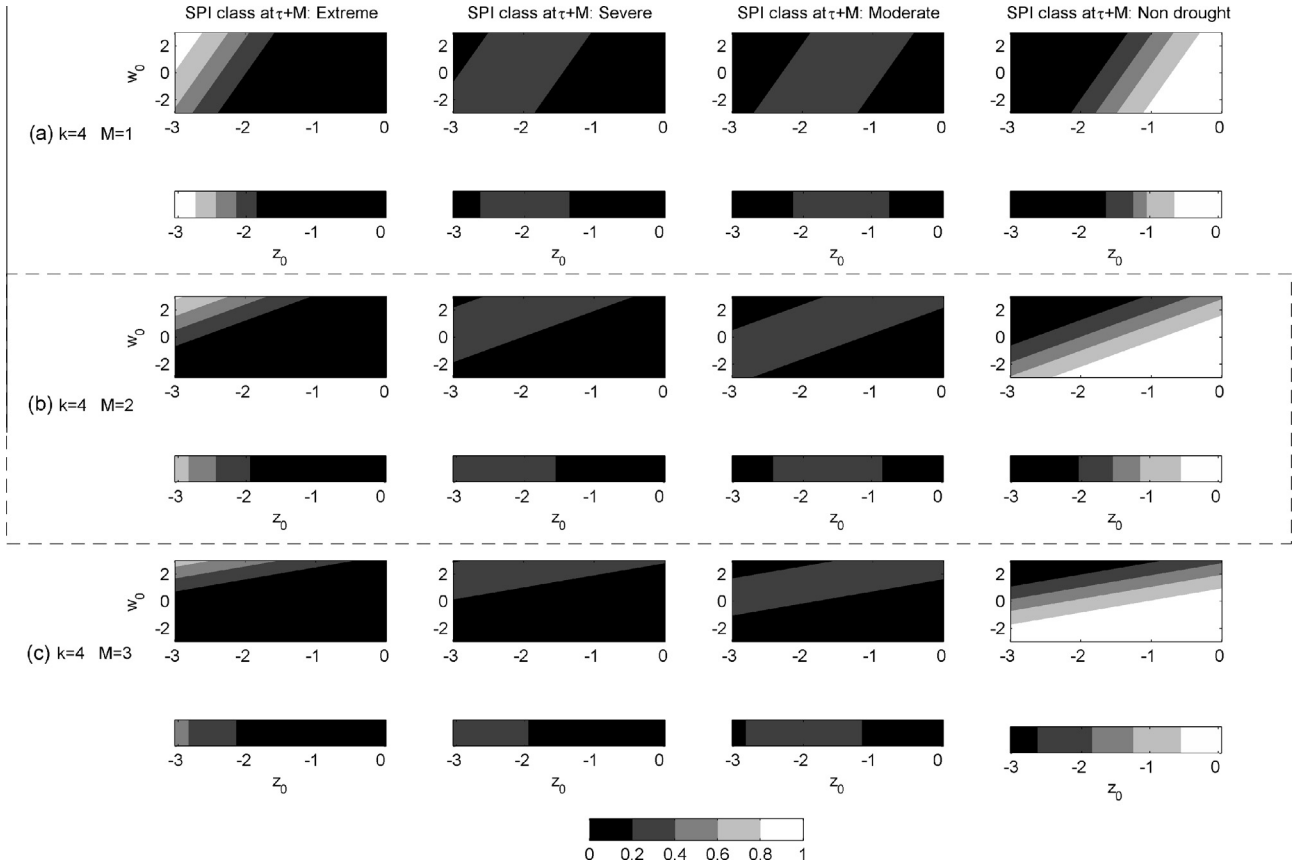

Fig. 6. As in Fig. 5 but for SPI-6 drought classes and March as current month τ.

Table 7
Transition probabilities from different current SPI-4 values to an extreme drought class M months ahead, with or without taking into account NAO (current month τ: February).

NAO value at February	SPI-4 value at February			
	$z_0 = -3.0$	$z_0 = -2.0$	$z_0 = -1.5$	$z_0 = -1.0$
Extreme drought class in March (M = 1 month)				
Without NAO	0.730	0.250	0.090	0.020
$w_0 = 3.0$	0.942	0.660	0.433	0.227
$w_0 = 0.0$	0.429	0.090	0.027	0.006
$w_0 = -3.0$	0.027	0.001	0.000	0.000
Extreme drought class in April (M = 2 months)				
Without NAO	0.435	0.168	0.087	0.039
$w_0 = 3.0$	0.811	0.614	0.498	0.381
$w_0 = 0.0$	0.110	0.035	0.017	0.008
$w_0 = -3.0$	0.000	0.000	0.000	0.000
Extreme drought class in May (M = 3 months)				
Without NAO	0.435	0.335	0.087	0.039
$w_0 = 3.0$	0.417	0.238	0.296	0.260
$w_0 = 0.0$	0.043	0.026	0.020	0.016
$w_0 = -3.0$	0.001	0.000	0.000	0.000

(top left smaller image), the most probable future class would always be Severe (Se) for $M = 1$ and $k = 4$ and 6 months and for $M = 2$ and $k = 6$ months, and Non drought (N) for $M = 2$ and $k = 4$ months and for $M = 3$ and $k = 4$ and 6 months.

As M increases the slope of the stripes decreases and Non Drought class (N) becomes more and more predominant with respect to the other classes, as the most probable future class.

4.4. Performance of the models

In order to quantitatively assess the skill in forecasting drought class transition probabilities of the proposed models, a simple score measure has been applied. In particular, following a procedure suggested by Chen et al. (2013), transition probabilities corresponding to SPI classes observed at month $\tau + M$ have been computed for each month of each year of the study period (1979–2008) by:

- Model 1: forecasting transition probability from class to class based on SPI class at month τ (Eq. (1)).
- Model 2: forecasting transition probability from class to class based on SPI and NAO classes at month τ (Eq. (2)).
- Model 3: forecasting transition probability from value to class based on SPI value at month τ (Eq. (9)).
- Model 4: forecasting transition probability from value to class based on SPI and NAO values at month τ (Eq. (16)).

Model calibration has been carried out according to a jackknife procedure (Miller, 1974). More specifically, let us consider a data matrix including n measured values of m predictor variables $X_{i,j}$, $i = 1, \ldots, n$ and $j = 1, \ldots, m$ (i.e. SPI at month τ or both SPI and NAO at month τ) and of a single criterion variable Y_i (i.e. SPI at month $\tau + M$). Therefore, the data matrix will have n rows and $m + 1$ columns. Then, the procedure consists in systematically removing one set of measurements from the data matrix and calibrating the model with the remaining $n - 1$ sets of measurements. The set of predictor measurements that is withheld at each step, is then used to predict transition probabilities to all the possible classes (Ex, Se, Mo and N) at month $\tau + M$.

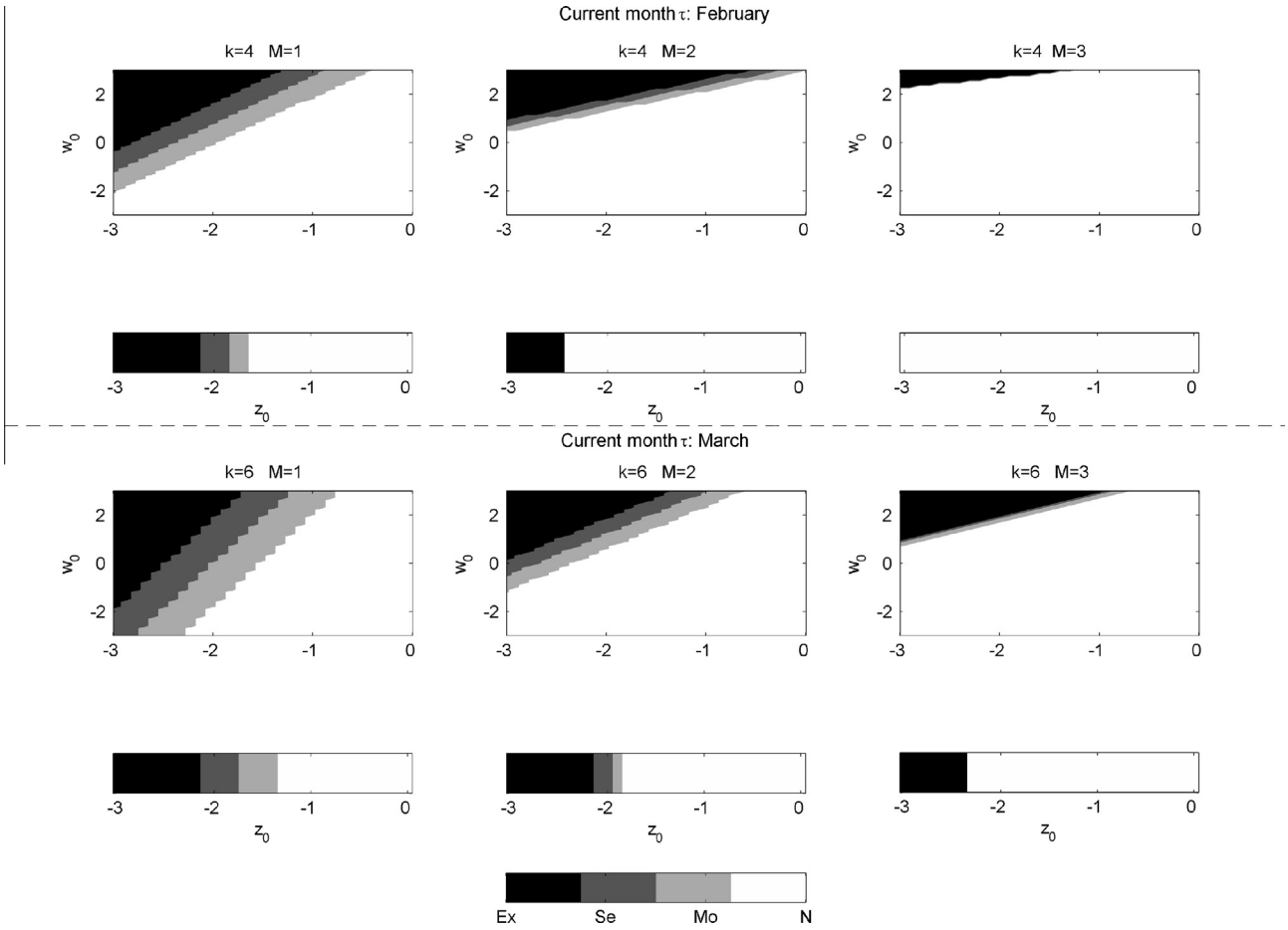

Fig. 7. Most probable transition classes of SPI-4 and SPI-6 for different time horizon M (current month τ: February and March, NAO AP = 4 months).

Table 8
Comparison of models scores (k = 4 months and M = 1, 2 and 3 months).

	Model 1 Eq. (1)	Model 2 Eq. (2)	Model 3 Eq. (9)	Model 4 Eq. (10)	Best model
M = 1	0.758	0.757	0.768	0.770	4
M = 2	0.727	0.727	0.733	0.738	4
M = 3	0.717	0.717	0.720	0.723	4

Table 9
Comparison of models scores (k = 6 months and M = 1, 2 and 3 months).

	Model 1 Eq. (1)	Model 2 Eq. (2)	Model 3 Eq. (9)	Model 4 Eq. (10)	Best model
M = 1	0.781	0.780	0.796	0.799	4
M = 2	0.738	0.738	0.748	0.751	4
M = 3	0.724	0.725	0.730	0.736	4

At this point, transition probability $p_{s,t}$ corresponding to the SPI class observed at month $t = \tau + M$ and year s, is retained as the score for that particular month and year. In practice, the highest score is given to the model which assigns the highest probability to the transition observed at month $\tau + M$.

In conclusion, the final model score S is determined as:

$$S = \frac{1}{12 \cdot n} \sum_{t=1}^{12} \sum_{s=1}^{n} p_{s,t} \tag{17}$$

Scores pertaining to each of the proposed models have been calculated and compared to evaluate the models' performance. The models scores S for M = 1, 2 and 3 months and k = 4 and 6 months are reported in Tables 8 and 9, respectively.

As it can be observed, Models 3 and 4 outperform Models 1 and 2 for every considered time horizon M. This confirms that forecasting SPI transition probabilities from a current value to a future class is more accurate than forecasting from class to class. Besides, Model 4 exhibits higher scores than the other models, implying that including NAO index as an exogenous variable can contribute to improve the performance of the forecasting model, mainly for short time horizons. On the other hand, including NAO index in forecasting transition probabilities from class to class does not seem to improve the model's performance, as the results of Model

1 and Model 2 are essentially the same for every M. The latter can be explained by the fact that almost all the observed pairs of current SPI and NAO classes, are those for which Model 1 and Model 2 forecast the same class at month $\tau + M$ as the most probable one (see, for instance, Table 5). Besides, it should be pointed out that performance of Model 2 are somewhat influenced by the choice of NAO classes intervals which is, indeed, arbitrary.

5. Conclusions

Several studies have shown that NAO exerts a strong influence on European climate. In the present paper the potential of NAO index to improve drought forecasting is analyzed with reference to Sicily region (Italy). In particular, two types of probabilistic forecasting models have been developed which express transition probabilities toward future SPI classes in analytical form, under the assumption of multivariate normal distribution of NAO and SPI series. The first type of models estimate transition probabilities from current classes to future classes, while the second ones evaluate transition probabilities from current values to future classes. Initially, only current SPI classes or values are considered, then the models are extended in order to include either current NAO classes or NAO values respectively, and compared with previous models.

A preliminary correlation analysis between NAO and SPI series, computed on areal monthly precipitation from 1979 until 2008, reveals higher negative correlations (with values generally less than -0.5) between NAO and SPI series during winter–spring season (generally from February to April).

With reference to transitions between drought classes, the statistical significance of NAO influence on future SPI classes has been tested by means of a Monte Carlo analysis, whose outcomes suggest that the effect of NAO on drought transition probabilities should be considered significant. Also, results indicate that transition probabilities toward equal or worse drought conditions increase as NAO tends toward extremely positive values, whereas probabilities toward less severe or to non-drought conditions decrease as NAO values increase for the considered SPI aggregation time scale k, time horizon M and NAO average period AP. As M increases, the influence of NAO becomes less significant when transition toward persisting or worse drought conditions are considered. A comparison among the most probable future SPI class resulting from the models, either by including or neglecting current NAO class, reveals that NAO influence decreases as the time horizon M increases, except for the case when extremely positive NAO class is considered.

The results of the model based on conditioning on a fixed SPI value indicate that more precise information on the most probable drought class in the future can be obtained in this case, since more details about current drought conditions are included in the model. Furthermore, including NAO within such model reveals that, on equal current SPI value, transition probabilities toward a future SPI drought class can change significantly according to the current NAO value.

Finally, a score measure based on probabilities corresponding to the observed SPI class at month $\tau + M$ has been applied to assess the skill in forecasting drought class transition probabilities of the proposed models. Scores of Model 4, which forecasts transition probabilities from current SPI and NAO values toward future classes, are higher than the ones of the other models for the considered time horizons M and aggregation time scales k. On the other hand Model 2, which forecasts transition probabilities from current SPI and NAO classes toward a future class, does not seem to provide a real improvement over the case when current NAO class is disregarded (Model 1).

Computation of drought transition probabilities can take advantage of analytical models, due to their ability to overcome the difficulties of more traditional approaches based on frequency analysis. Indeed, the limited numbers of transitions usually observed on even long historical series can lead to unreliable estimation of related probabilities by means of an inferential approach. Moreover, analytical models enable to take into account information from exogenous variables exerting influence on the climate of the study area, such as NAO, thus leading to a more accurate prediction of drought class transitions.

The proposed models can be easily extended to different drought indices, as for instance the Standardized Precipitation Evapotranspiration Index (SPEI) by Vicente-Serrano et al. (2010), as well as to other large scale atmospheric patterns properly selected according to the climate features of the study area.

References

Bacanli, U., Firat, M., Dikbas, F., 2009. Adaptive neuro-fuzzy inference system for drought forecasting. Stochast. Environ. Res. Risk Assess. 23, 1143–1154.

Barua, S., Ng, A., Perera, B., 2012. Artificial neural network based drought forecasting using a nonlinear aggregated drought index. J. Hydrologic Eng. 17 (12), 1408–1413.

Belayneh, A., Adamowski, J., Khalil, B., Ozga-Zielinski, B., 2014. Long-term SPI drought forecasting in the Awash River Basin in Ethiopia using wavelet neural networks and wavelet support vector regression models. J. Hydrol. 508, 418–429.

Bonaccorso, B., Bordi, I., Cancelliere, A., Rossi, G., Sutera, A., 2003. Spatial variability of drought: an analysis of SPI in Sicily. Water Resour. Manage. 17, 273–296.

Bonaccorso, B., Cancelliere, A., Rossi, G., 2012. Methods for drought analysis and forecasting. In: Balakrishnan, N. (Ed.), Methods and Applications of Statistics in the Atmospheric and Earth Sciences. John Wiley and Sons, Hoboken, pp. 150–184.

Brandimarte, L., Di Baldassarre, G., Bruni, G., D'Odorico, P., Montanari, A., 2011. Relation between the North-Atlantic Oscillation and hydroclimatic conditions in Mediterranean areas. Water Resour. Manage. 25 (5), 1269–1279.

Brunetti, M., Maugeri, M., Monti, F., Nanni, T., 2006. Temperature and precipitation variability in Italy in the last two centuries from homogenized instrumental time series. Int. J. Climatol. 26 (3), 345–381.

Cancelliere, A., Di Mauro, G., Bonaccorso, B., Rossi, G., 2007. Drought forecasting using the Standardized Precipitation Index. Water Resour. Manage. 21 (5), 801–819.

Chen, S.T., Yang, T.C., Kuo, C.M., Kuo, C.H., Yu, P.S., 2013. Probabilistic drought forecasting in Southern Taiwan using El Niño-Southern Oscillation index. Terr. Atmos. Ocean. Sci. 24, 911–924.

Cullen, H.M., deMenocal, P.B., 2000. North Atlantic influence on Tigris-Euphrates streamflow. Int. J. Climatol. 20, 853–863.

Cutore, P., Di Mauro, G., Cancelliere, A., 2009. Forecasting palmer index using neural networks and climatic indexes. J. Hydrol. Eng. 14 (6), 588–595.

Di Mauro, G., 2006. Stochastic Forecasting of Drought: Application to SPI index, Ph. D. Dissertation, Department of Civil and Environmental Engineering, University of Catania (in Italian).

Durdu, O., 2010. Application of linear stochastic models for drought forecasting in the Basilisk Menderes river basin, Western Turkey. Stochast. Environ. Res. Risk Assess. 24, 1145–1162.

Farokhnia, A., Morid, S., Byun, H.R., 2011. Application of global SST and SLP data for drought forecasting on Tehran plain using data mining and anfis techniques. Theor. Appl. Climatol. 104, 71–81.

Fernandez, C., Vega, J., Fonturbel, T., Jimenez, E., 2009. Streamflow drought time series forecasting: a case study in a small watershed in NorthWest Spain. Stochast. Environ. Res. Risk Assess. 23, 1063–1070.

Ferrari, E., Caloiero, T., Coscarelli, R., 2013. Influence of the North Atlantic Oscillation on winter rainfall in Calabria (southern Italy). Theor. Appl. Climatol. 114 (3–4), 479–494.

Fetter, C.W., 1994. Applied Hydrogeology. Macmillan College Publishing Co., New York.

Gabriel, K., Neumann, J., 1962. A Markov chain model for daily rain occurrences at Tel Aviv. Quart. Royal Meteorol. Soc., 88

Gimeno, L., Ribera, P., Iglesias, R., De la Torre, L., García, R., Hernández, E., 2002. Identification of empirical relationships between indices of ENSO and NAO and agricultural yields in Spain. Clim. Res. 21, 165–172.

Goodess, C.M., Jones, P.D., 2002. Links between circulation and changes in the characteristics of Iberian rainfall. Int. J. Climatol. 22, 1593–1615.

Han, P., Wang, P., Zhang, S., Zhu, D., 2010. Drought forecasting based on the remote sensing data using ARIMA models. Mathemat. Comput. Model. 51, 1398–1403.

Hayes, M.J., Svoboda, M., Wilhite, D.A., Vanyarkho, O., 1999. Monitoring the 1996 drought using the SPI. Bull. Am. Meteorol. Soc. 80, 429–438.

Helsel, D.R., Hirsh, R.M., 1992. Statistical Methods in Water Resources, Studies in Environmental Sciences, vol. 49. Elsevier, New York.

Hurrell, J.W., 1995. Decadal trends in the North Atlantic Oscillation: Regional temperatures and precipitation. Science 7, 676–679.

Hurrell, J.W., Van Loon, H., 1997. Decadal variations in climate associated with the North Atlantic Oscillation. Clim. Chang. 36, 301–326.
Hurrell, J.W., Kushnir, Y., Visbeck, M., 2001. The North Atlantic Oscillation. Science 291 (5504), 603–605.
Hurrell, J.W., Kushnir, Y., Ottersen, G., Visbeck, M., 2003. An overview of the North Atlantic Oscillation. In: The North Atlantic Oscillation: Climate Significance and Environmental Impact, Geophys. Monogr, vol. 134. Am. Geophys. Union, pp. 1–36.
Jamshidi, H., Arian, A., Rezaeian-Zadeh, M., 2011. Drought forecasting by multi layer perceptron network in different climatology regions. In: Proc. ICID 21st International Congress on Irrigation and Drainage, Tehran, Iran, 15–23 October 2011.
Jones, P.D., Jonsson, T., Wheeler, D., 1997. Extension of the North Atlantic Oscillation using early instrumental pressure observations from Gibraltar and southwest Iceland. Int. J. Climatol. 17, 1433–1450.
Kavalieratou, S., Karpouzos, D.K., Babajimopoulos, C., 2012. Drought analysis and short-term forecast in the Aison River Basin (Greece). Nat. Hazard. Earth Syst. Sci. 12 (5), 1561–1572.
Kim, T., Valdes, J.B., 2003. Nonlinear model for drought forecasting based on a conjunction of wavelet transforms and neural networks. J. Hydrol. Eng. 8 (6), 319–328.
Lohani, V., Loganathan, G., 1997. An early warning system for drought management using the Palmer Drought Index. J. Am. Water Resources Assoc. 33, 1375–1386.
Lohani, V.K., Loganathan, G.V., Mostaghimi, S., 1998. Long-term analysis and short-term forecasting of dry spells by Palmer Drought Severity Index. Nord. Hydrol. 29 (1), 21–40.
Lopez-Moreno, J.I., Vicente-Serrano, S., 2008. Extreme phases of the wintertime North Atlantic Oscillation and drought occurrence over Europe: a multi-temporal scale approach. J. Clim. 21, 1220–1243.
Lopez-Moreno, J.I., Beguerìa, S., Vicente-Serrano, S.M., Garcìa-Ruiz, J.M., 2007. Influence of the North Atlantic Oscillation on water resources in central Iberia: precipitation, streamflow anomalies, and reservoir management strategies. Water Resour. Res. 43, W09411.
Mardia, K.V., 1970. Measures of multivariate skewness and kurtosis with applications. Biometrika 57 (3), 519–530.
McKee, T.B., Doesken, N.J., Kleist, J., 1993. The relationship of drought frequency and duration to time scales. In: Proc. 8th Conference on Applied Climatology, Anaheim, California, pp. 179–184.
Miller, R.G., 1974. The Jackknife – a review. Biometrika 61 (1), 1–15.
Mishra, A., Desai, V., 2005. Spatial and temporal drought analysis in the Kansabati river basin, India. Int. River Basin Manage. 3, 31–41.
Mishra, A., Desai, V., 2006. Drought forecasting using feed-forward recursive neural network. Ecol. Model. 198, 127–138.
Mishra, A., Desai, V., Singh, V., 2007. Drought forecasting using a hybrid stochastic and neural network model. J. Hydrol. Eng. 12, 626–638.
Modarres, R., 2007. Streamflow drought time series forecasting. Stochastic Environ. Res. Risk Assess. 21, 223–233.
Mood, A.M., Graybill, F.A., Boes, D., 1988. Introduction to the Theory of Statistics. McGraw-Hill, New York.
Moreira, E.E., Paulo, A.A., Pereira, L.S., Mexia, J.T., 2006. Analysis of SPI drought class transitions using loglinear models. J. Hydrol. 331 (1–2), 349–359.
Moreira, E.E., Coelho, C.A., Paulo, A.A., Pereira, L.S., Mexia, J.T., 2008. SPI-based drought category prediction using loglinear models. J. Hydrol. 354 (1–4), 116–130.
Morid, S., Smakhtin, V., Bagherzadeh, K., 2007. Drought forecasting using artificial neural networks and time series of drought indices. Int. J. Climatol. 27, 2103–2111.
Muñoz-Diaz, D., Rodrigo, F.S., 2004. Impacts of the North Atlantic Oscillation on the probability of dry and wet winters in Spain. Climate Res. 27, 33–43.
Namias, J., 1985. Factors responsible for the droughts. In: Beran, M.A., Rodier, J.A. (Eds.), Hydrologic Aspects of Drought, UNESCO – World Meteorological Organization, Paris, pp. 27–64 (Chapter 3).
Osborn, T.J., Briffa, K.R., Tett, S.F.B., Jones, P.D., Trigo, R.M., 1999. Evaluation of the North Atlantic oscillation as simulated by a climate model. Clim. Dyn. 15, 685–702.
Ozger, M., Mishra, A., Singh, V., 2012. Long lead time drought forecasting using a wavelet and fuzzy logic combination model: a case study in Texas. J. Hydrometeorol. 13, 284–297.
Palmer, W.C., 1965. Meteorological Drought, Research Paper, 45, U.S. Weather Bureau.
Paulo, A., Pereira, L., 2007. Prediction of SPI drought class transitions using Markov chains. Water Res. Manage. 21, 1813–1827.
Paulo, A., Ferreira, E., Coelho, C., Pereira, L., 2005. Drought class transition analysis through Markov and Loglinear models, an approach to early warning. Agric. Water Manage. 77, 59–81.
Rao, A.R., Padmanabhan, G., 1984. Analysis and modelling of Palmer's drought index series. J. Hydrol. 68, 211–229.
Rogers, J.C., 1984. The association between the North Atlantic Oscillation and the Southern Oscillation in the Northern Hemisphere. Mon. Weather Rev. 112, 1999–2015.
Ropelewski, C.F., Halpert, M.S., 1987. Global and regional scale precipitation patterns associated with the El Niño/Southern Oscillation. Mon. Weather Rev. 115, 1606–1626.
Rossi, G., 2003. Requisites for a drought watch system. In: Rossi, G. et al. (Eds.), Tools for Drought Mitigation in Mediterranean Regions. Kluwer Academic Publishing, Dordrecht, pp. 147–157.
Santos, J.F., Portela, M.M., Pulido-Calvo, I., 2014. Spring drought prediction based on winter NAO and global SST in Portugal. Hydrol. Process. 28 (3), 1009–1024.
Schervish, M.J., 1984. Algorithm AS 195. multivariate normal probabilities with error bound. Appl. Stat. 33 (1), 81–94.
Thiessen, A.H., 1911. Precipitation for large areas. Mon. Weather Rev. 39, 1082–1084.
Trigo, R.M., Osborn, T.J., Corte-Real, J.M., 2002. The North Atlantic Oscillation influence on Europe: Climate impacts and associated physical mechanisms. Climate Res. 20, 9–17.
Türkes, M., Erlat, E., 2003. Precipitation changes and variability in Turkey linked to the North Atlantic Oscillation during the period 1930–2000. Int. J. Climatol. 23, 1771–1796.
Van der Schrier, G., Briffa, K.R., Jones, P.D., Osborn, T.J., 2006. Summer moisture variability across Europe. J. Climate 19, 2818–2834.
Vicente-Serrano, S.M., Beguería, S., López-Moreno, J.I., 2010. A multiscalar drought index sensitive to global warming: the Standardized Precipitation Evapotraspiration Index. J. Climate 23, 1696–1718.
Vicente-Serrano, S.M., López-Moreno, J.I., Lorenzo-Lacruz, J., El Kenawy, A., Azorin-Molina, C., Morán-Tejeda, E., Pasho, E., Zabalza, J., Beguería, S., Angulo-Martínez, M., 2011. The NAO impact on droughts in the Mediterranean region. In: Vicente-Serrano, S.M., Trigo, R.M. (Eds.), Hydrological, Socioeconomic and Ecological Impacts of the North Atlantic Oscillation in the Mediterranean Region, Advances in Global Change Research, vol. 46. Springer, Dordrecht.
Walker, G.T., Bliss, E.W., 1932. World Weather V. Mem. Roy. Met. Soc. 4, 53–84.
Wang, G.A., Dolman, J., Alessandri, A., 2011. A summer climate regime over Europe modulated by the North Atlantic Oscillation. Hydrol. Earth Syst. Sci. 15, 57–64.
Wedgbrow, C.S., Wilby, R.L., Fox, H.R., O'Hare, G., 2002. Prospects for seasonal forecasting of summer drought and low river flow anomalies in England and Wales. Int. J. Climatol. 22 (2), 219–236.
World Meteorological Organization, 2011. Sixteenth World Meteorological Congress. Abridged Final Report with Resolutions. WMO-No. 1077. Geneva, 16 May–3 June 2011.